Discover Oncology

Research

CAT and CXCL8 are crucial cofactors for the progression of nonalcoholic steatohepatitis to hepatocellular carcinoma, the immune infiltration and prognosis of hepatocellular carcinoma

Liang Yang[1] · Peiping Li[1] · JiaLi Zhao[1] · Zirui Bai[1] · Guifang Zeng[1] · Xialei Liu[1] · Baojia Zou[1] · Jian Li[1]

Received: 3 November 2024 / Accepted: 4 March 2025
Published online: 07 March 2025

Abstract

Purpose Hepatocellular carcinoma (HCC) is a malignant tumour characterized by high morbidity and mortality. Immunotherapy is an important treatment newly approved for the treatment for advanced hepatocellular carcinoma. However, how NASH progresses to HCC and the association between the immune signature in HCC and patient prognosis remain unclear.

Methods Data from NASH and NASH-HCC patients were obtained from the GEO database. Differentially expressed genes were screened and hub genes were identified. The enrichment analysis, clustering, cibersort, ssGSEA, Xcell and immune checkpoint expression data of the samples were analysed. Survival analysis of dual genes was performed using TCGA liver cancer samples and the lasso regression model, and Cox regression analysis was conducted. Pathology specimens from 21 NASH-associated hepatocellular carcinoma patients were collected, and immunohistochemical staining was used to verify gene expression.

Results Compared with HCC patients with high CAT and low CXCL8 expression, those with low CAT and high CXCL8 expression had significantly higher levels of infiltration of multiple immune cell types and the common immune checkpoints CD274, PDCD1 and CTLA4. Furthermore, CAT was a protective factor, and CXCL8 was a risk factor for the prognosis of HCC patients.

Conclusion CAT and CXCL8 might impact NASH-HCC progression. HCC patients with low CAT and high CXCL8 expression might have more extensive immune cell infiltration and stronger tumour immune escape. However, probably due to their different effects on CD8 + T cells and reactive oxygen species, increased expression of CAT contributes to improved prognosis in HCC patients, whereas increased expression of CXCL8 leads to a poor prognosis.

Keywords Nonalcoholic steatohepatitis · Hepatocellular carcinoma · Immunotherapy · Prognosis

Liang Yang, Peiping Li and JiaLi Zhao contributed equally.

✉ Xialei Liu, liuxlei3@mail.sysu.edu.cn; ✉ Baojia Zou, zoubj6@mail.sysu.edu.cn; ✉ Jian Li, lijian5@mail.sysu.edu.cn; Liang Yang, yangliang9@mail2.sysu.edu.cn | [1]Department of Hepatobiliary Surgery, The Fifth Affiliated Hospital of Sun Yat-Sen University, 52 Mei Hua East Road, Zhuhai 519000, Guangdong Province, China.

1 Introduction

Hepatocellular carcinoma (HCC) is the fifth most prevalent cancer and the third leading cause of cancer-related mortality [1]. The World Health Organization (WHO) predicts that HCC will result in more than one million deaths by 2030 [2]. There are a myriad of potential aetiologies for HCC, including hepatitis B virus or hepatitis C virus infection, excessive alcohol consumption, nonalcoholic fatty liver disease (NAFLD), aflatoxin, and insidious cirrhosis. Among these causes, NAFLD has emerged as a cause of the disease in recent decades. However, there is still a lack of in-depth understanding of the carcinogenic mechanisms involved in NAFLD, which could lead to different treatment strategies [3–5].NAFLD is a general term for a series of diseases, including simple steatosis, nonalcoholic fatty liver disease, and nonalcoholic steatohepatitis (NASH), leading to eventual liver cirrhosis and HCC (pathologically known as NASH-HCC) [6–8].

Compared with targeted therapy alone, targeted therapy combined with immunotherapy is currently considered a first-line treatment for advanced liver cancer, and the effect is significantly improved; for example, combined therapy with atezolizumab (an anti-PD-1 monoclonal antibody) and bevacizumab (an anti-VEGF monoclonal antibody) has demonstrated enhanced therapeutic effects. However, the objective response rate (ORR) of this combined therapy remains limited to no more than 30% [9, 10]. Additionally, nonviral HCC, particularly NASH-HCC, may have a lower response rate to immunotherapy than virus-related HCC [11], which makes NASH-HCC a more challenging tumour to treat despite the increase in immunotherapy. Numerous studies have explored the relationships between the progression of NASH-HCC and immune cells. Dysregulated intrahepatic CD8 + T cells and natural killer T (NKT) cells have been implicated in the induction of NASH-HCC in a mouse model [12]. Liver-specific Kupffer cells (the resident macrophages of the liver) are not only potential therapeutic targets for NASH-HCC, but also drivers of the development of HCC [13–15]. Furthermore, tumour heterogeneity is closely associated with the complicated immune microenvironment and affects treatment sensitivity to immunotherapy [16, 17]. However, how NASH progresses into liver cancer and the associations between immune signatures in HCC and patient prognosis remain largely unknown.

CAT is an enzyme that decomposes hydrogen peroxide, a reactive oxygen species (ROS) that plays a crucial role in regulating cell function. The role of ROS in cancer is still poorly understood, and the existing evidence remains controversial. Tumour cells can produce large amounts of ROS, which cause damage to DNA, proteins, and lipids, leading to carcinogenesis [18, 19]. Moreover, CAT can induce certain cells in the tumour immune microenvironment, such as CD8 + T cells, to enhance the antitumour immune response [20].

The chemokine CXCL8 (also known as IL-8) belongs to the CXC family and plays a crucial role in recruiting various immune cells to inflammatory sites. Additionally, CXCL8 promotes angiogenesis and the synthesis of matrix metalloproteinases (MMPs), which promote tissue remodelling after metastasis [21–24]. High expression of CXCL8 is associated with increased cancer risk and poor prognosis [25, 26]. Within the tumour immune microenvironment, CXCL8 can directly or indirectly affect multiple immune cells, including dendritic cells and central granulocytes, trigger complicated immune responses and even hamper antitumour immunity [27]. Previous studies have suggested a potential relationship between disturbances in CAT and CXCL8 expression in small intestinal epithelial cells for regulating immune cell infiltration [28], but their specific associations in HCC remain unknown.

Therefore, this study aimed to identify crucial genes involved in the development and progression of nonalcoholic steatohepatitis-associated HCC (NASH-HCC) by comparing differential gene expression between NASH-HCC and nonalcoholic steatohepatitis samples. In this study, CXCL8 and CAT were identified as crucial cofactors in NASH-HCC development and were subsequently validated in paraffin-embedded samples from NASH-HCC patients at our centre. Furthermore, we aimed to investigate the relationships between the expression levels of crucial genes and immune infiltration characteristics as well as patient survival time in patients with HCC.

2 Materials and methods

2.1 Expression matrix data processing and differential analysis

The GSE164760 [29]expression matrix was downloaded from the GEO database (https://www.ncbi.nlm.nih.gov/geo/), which included a total of 74 NASH samples and 53 NASH-HCC samples. The limma package in R was used to

standardize the expression matrix and perform differential analysis to obtain differentially expressed genes (DEGs), log FC (fold change) > 1 and p value < 0.05 was considered to indicate statistical significance. The pheatmap package in R was used to draw the difference analysis heatmap, and the ggpubr package and ggthemes package were used to draw the volcano map.

2.2 GO and KEGG enrichment analysis of DEGs

The clusterProfiler package in R was used to perform GO and KEGG analyses of the DEGs to explore the potential biological processes and signalling pathways involved in the development of NASH-HCC.

2.3 Establishment of the PPI network and screening of hub genes

An online database (https://cn.string-db.org/) was used to construct the protein–protein interaction (PPI) network of the DEGs, and the minimum required interaction score was set as medium confidence (0.400) [30–32]. The network was beautified and analysed using Cytoscape 3.7.2, and the hub genes in the interaction network were obtained by the degree algorithm and MNC algorithm using the cytoHubba tool. The degree algorithm evaluates the importance according to the number of connections of gene nodes. The higher the degree value is, the greater the degree of interaction the gene has. The MNC algorithm identifies the connectivity and influence of each gene in its neighbouring gene nodes. The higher the MNC score is, the greater the influence of the gene on its neighbouring nodes.

2.4 Survival analysis and lasso regression model of the hub genes

GEPIA is a web-based tool that provides fast and customizable functionality using TCGA and GTEx data [33]. Survival analysis of the hub genes was performed using the online database GEPIA (http://gepia.cancer-pku.cn/) to evaluate the correlation between the expression of the hub genes and the prognosis of hepatocellular carcinoma patients. Then, using the ConsensusClusterPlus package, the 363 tumour samples with survival data in TCGA were clustered according to the hub genes, and survival analysis was performed again to verify the results. Univariate and multivariate Cox regression analyses were also conducted. The risk score was calculated, and a least absolute shrinkage and selection operator (lasso) model was established to evaluate the prognostic effectiveness of hub gene expression.

2.5 Analysis of the effects of the hub genes on immune infiltration in hepatocellular carcinoma

The proportions of immune cells in 53 NASH-HCC samples were visualized using cibersort in R. To analyse the influence of the hub genes on the immune infiltration of NASH-HCC, the 53 NASH-HCC tumour samples and TCGA HCC samples were classified into two subgroups according to the expression of the hub genes using the ConsensusClusterPlus package and a corresponding heatmap was drawn. The estimate package in R was used to calculate the immune score, stromal score, ESTIMATE score and tumour purity of 53 NASH-HCC samples, and the patients were grouped and compared according to the tumour subgroups after clustering. The differences in immune infiltration among tumour subgroups were analysed using the GSVA package (ssGSEA) and Xcell package in R.

2.6 Exploration of the effects of hub genes on immune checkpoint expression and immunotherapy effects

The 363 liver cancer samples with survival data in the TCGA database and 53 NASH-HCC samples were classified according to tumour subgroup to analyse the differences in the expression of PDCD1, CD274 and CTLA4, and to explore the effects of the hub genes on liver cancer immunotherapy. The TIDE (Tumour Immune Dysfunction and Exclusion) database integrates 33,197 tumour samples from 189 human cancer studies to simulate the immune evasion status of tumours by hypothesizing and validating precise gene markers, thereby predicting the response to immune therapy for tumours. The Dysfunction score reflects the ability of the tumour to impair the function of cytotoxic T lymphocytes; the Exclusion score reflects the ability of the tumour to prevent the infiltration of cytotoxic T lymphocytes; the TIDE score is the sum of the Dysfunction and Exclusion scores, and a higher TIDE score indicates that the tumour is more prone to immune evasion, and the immune therapy effect may not be ideal; the MSI score is evaluated based on the correlation between microsatellite instability status and the effect of immune therapy, and a lower MSI score suggests a stronger ability of the tumour to evade immune therapy, and a

worse effect of immune therapy [34]. The liver cancer samples from TCGA were analysed in the TIDE database to predict the immune therapy effect between tumour subgroups.

2.7 Immunohistochemical staining and analysis of CAT/CXCL8 in NASH patients and NASH-HCC patients from our centre

A total of 10 NASH samples and a total of 21 NASH-HCC samples from our centre were analysed by immunohistochemical staining. Following the removal of paraffin by xylene and ethyl alcohol, sodium citrate repair solution was used to repair antigen damage, after which endogenous peroxidase was inactivated with 3% hydrogen peroxide. The NAFLD and NAFLD-HCC sections were exposed to primary antibodies against CAT (1:1000; 66765–1-IG; Proteintech, Guangzhou, China) and CXCL8 (1:400; 27095-1-AP; Proteintech, Guangzhou, China) at 4 ℃ overnight, followed by washing with phosphate buffered saline (PBS). The sections were subsequently incubated with secondary antibodies (anti-mouse/rabbit IgG; Boster, Wuhan, China) for 30 min. The slides were subsequently coloured with DAB (DAB substrate:DAB concentrate = 1 ml:50 µl) and haematoxylin (Biosharp, Shanghai, China). Stained images were taken, and 10 regions were chosen randomly from each stained image. ImageJ software was used to calculate the immunohistochemical staining intensity of each region, and the mean value was calculated as the hub gene expression level.

2.8 Statistical analysis

All bioinformatics analyses were performed using R4.2.2. The experimental data were analysed and visualized using GraphPad Prism 8. Univariate and multivariate Cox regression analyses were also used to assess the relationships between the clinical characteristics and overall survival of patients. The area under the ROC curve (AUC) was used as an index to assess the accuracy of the genetic signature risk score in predicting survival. In all analyses, a p value of < 0.05 was considered to indicate statistical significance.

3 Result

3.1 Volcano maps and heatmaps revealed significantly differentially expressed genes between NASH and NASH-HCC patients

The dataset GSE164760 was retrieved from the GEO database, and the details of the dataset are listed in Table 1. The dataset included sequencing data from samples of 74 NASH patients and 53 NASH-HCC patients. After normalization of the expression matrix, a total of 33 upregulated genes and 77 downregulated genes were screened between NASH and NASH-HCC patients. The expression heatmap of the DEGs is shown in Fig. 1A, and the volcano map is shown in Fig. 1B.

3.2 GO and KEGG enrichment analyses of DEGs in NASH-HCC

To further explore the potential biological processes and signalling pathways involved in the progression of NASH-HCC, we first performed GO enrichment analysis and KEGG analysis of 110 DEGs. The GO analysis results are shown in Fig. 2A. The top 10 biological processes with the highest P value enriched in the biological process (BP) category included the xenobiotic stimulus, hormone metabolic process, olefinic compound metabolic process, cellular hormone metabolic process, detoxification, cellular response to xenobiotic stimulus, terpenoid metabolic process, isoprenoid metabolic process, detoxification of inorganic compound, detoxification of copper ion. Moreover, according to the logFC absolute value, the top 5 biological processes enriched in the genes with the most significant expression differences in NASH-HCC patients were olefinic compound metabolic process, detoxification of inorganic compound, response to xenobiotic stimulus, cellular response to xenobiotic stimulus, and hormone metabolic process (Fig. 2B**)**. The top 10 signalling pathway with the highest P value obtained using KEGG enrichment analysis are shown in Fig. 2C. These pathways included drug metabolism—cytochrome P450, carbon metabolism, retinol metabolism, chemical

Table 1 Details of the GEO NASH and NASH-HCC data

Reference	GEO	Platform	NASH	NASH-HCC
Pinyol R (2021)	GSE164760	GPL13667	74	53

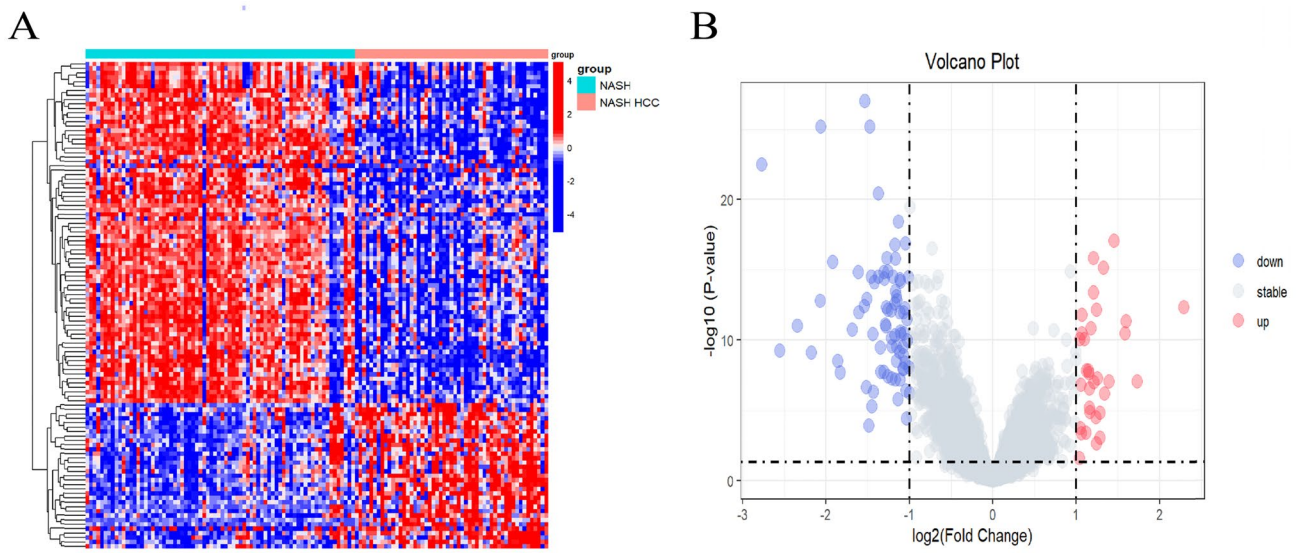

Fig. 1 **A** Heatmap of DEGs in NASH (N = 74) and NASH-HCC (N = 53) patients. **B** Volcano plots of DEGs in patients with NASH (N = 74) and patients with NASH-HCC (N = 53). A total of 33 upregulated genes and 77 downregulated genes were identified. Red indicates upregulated genes and blue indicates downregulated genes

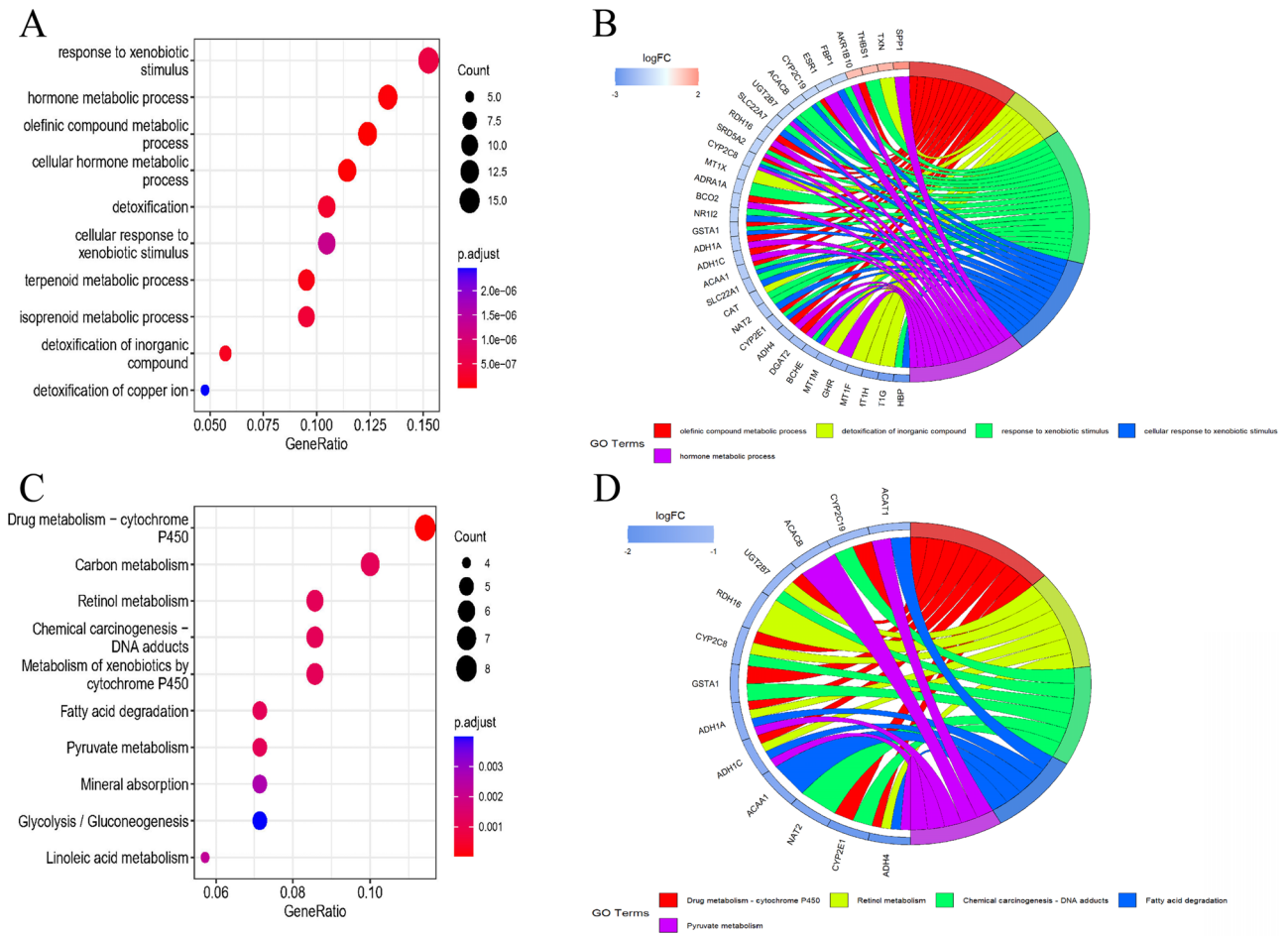

Fig. 2 **A, B** Results of the GO enrichment analysis. **C, D** Results of the KEGG enrichment analysis

carcinogenesis—DNA adducts, metabolism of xenobiotics by cytochrome P450, fatty acid degradation, pyruvate metabolism, mineral absorption, glycolysis/gluconeogenesis, and linoleic acid metabolism. The top 5 signalling pathways enriched with the highest logFC absolute value in DEGs were drug metabolism—cytochrome P450, retinol metabolism, chemical carcinogenesis—DNA adducts, fatty acid degradation, and pyruvate metabolism (Fig. 2D**)**. Most of the biological processes and pathways associated with the DEGs were related to metabolism. Among them, the response to xenobiotic stimulus, cellular response to xenobiotic stimulus, Chemical carcinogenesis—DNA adducts are known to be closely related to tumorigenesis.

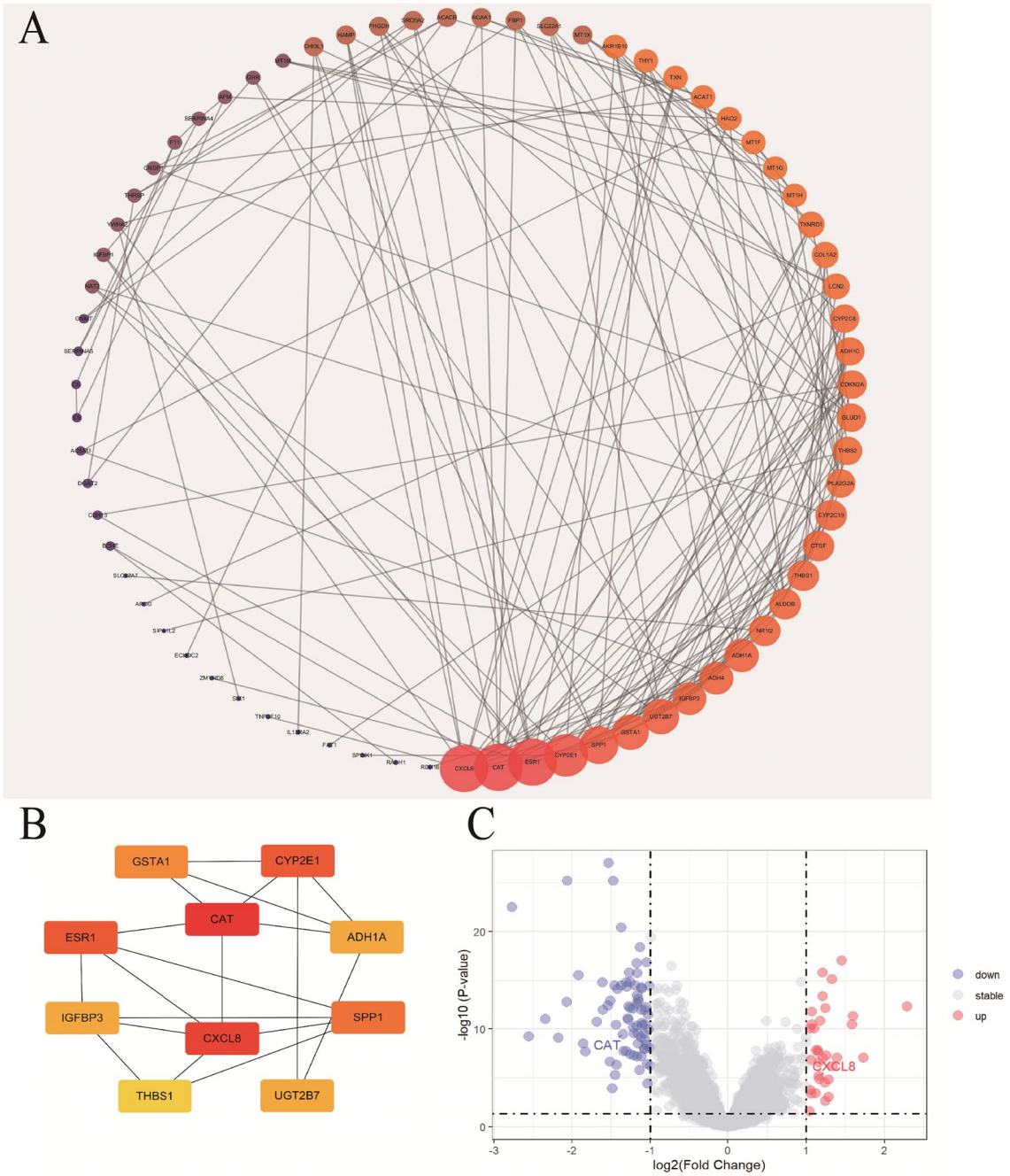

Fig. 3 **A** PPI network diagram. **B** The top ten genes according to the MNC algorithm; **C** Expression of CAT and CXCL8 among the DEGs

Table 2 Degree values of the hub genes

Rank	Gene	Degree value
1	CXCL8	15
1	CAT	15
1	ESR1	15
4	CYP2E1	13
5	SPP1	11
6	UGT2B7	10
6	GSTA1	10
8	IGFBP3	9
8	ADH4	9
8	ADH1A	9

Table 3 MNC scores of the hub genes

Top10 in PPI network ranked by MNC method			
Rank	Gene	Score	Differential expression
1	CAT	14	Down
2	CXCL8	13	Up
3	ESR1	12	Down
4	CYP2E1	12	Down
5	SPP1	11	Up
6	GSTA1	10	Down
7	IGFBP3	9	Down
8	ADH1A	9	Down
9	UGT2B7	9	Down
10	THBS1	8	Up

3.3 PPI network and hub genes among the DEGs of NASH-HCC patients

Protein–protein interaction (PPI) analysis was subsequently performed on the 110 DEGs in the string database, and the results were imported into Cytoscape 3.7.2 to construct a ring diagram (Fig. 3A). Degree algorithm refers to the number of connections between a gene and other genes, and a higher degree value often means that the role of this gene is more important. The PPI network was visualized according to the degree value; a brighter colour meant a larger degree value, a larger circle meant a larger degree value, CAT, CXCL8, ESR1, etc. (Table 2) had significant degree values. The top ten hub genes identified using MNC algorithm in cytoHubba are shown in Fig. 3B. Details of the hub genes are provided in Table 3. As shown in Fig. 3C and Table 3, CAT was the highest ranked downregulated gene, and CXCL8 was the highest ranked upregulated gene. In this way, we propose that CAT and CXCL8 might play key roles in the progression of NASH to HCC.

3.4 CAT and CXCL8 are crucial factors in predicting HCC patient survival

To further explore the effects of CAT and CXCL8 expression levels on patients with liver cancer, single-gene survival analysis of CAT and CXCL8 in HCC was performed using the GEPIA database. The HR of CAT was 0.63, and the p(HR) = 0.011, indicating that CAT was a protective factor against the progression of liver cancer (Fig. 4A). Survival analysis of the TCGA HCC samples was also conducted. The survival time of the high CAT group (median survival time/MST = 70.1 months) was significantly better than that of the low CAT group (MST = 41.8 months) (Fig. 4B).

On the other hand, the HR of CXCL8 was 1.6 (high expression vs. low expression), p(HR) = 0.012, indicating that CXCL8 was a risk factor for the progression of HCC patients (Fig. 4C). The survival time of the high CXCL8 group (MST = 45.1 months) was significantly worse than that of the low CXCL8 group (MST = 81.7 months) (Fig. 4D).

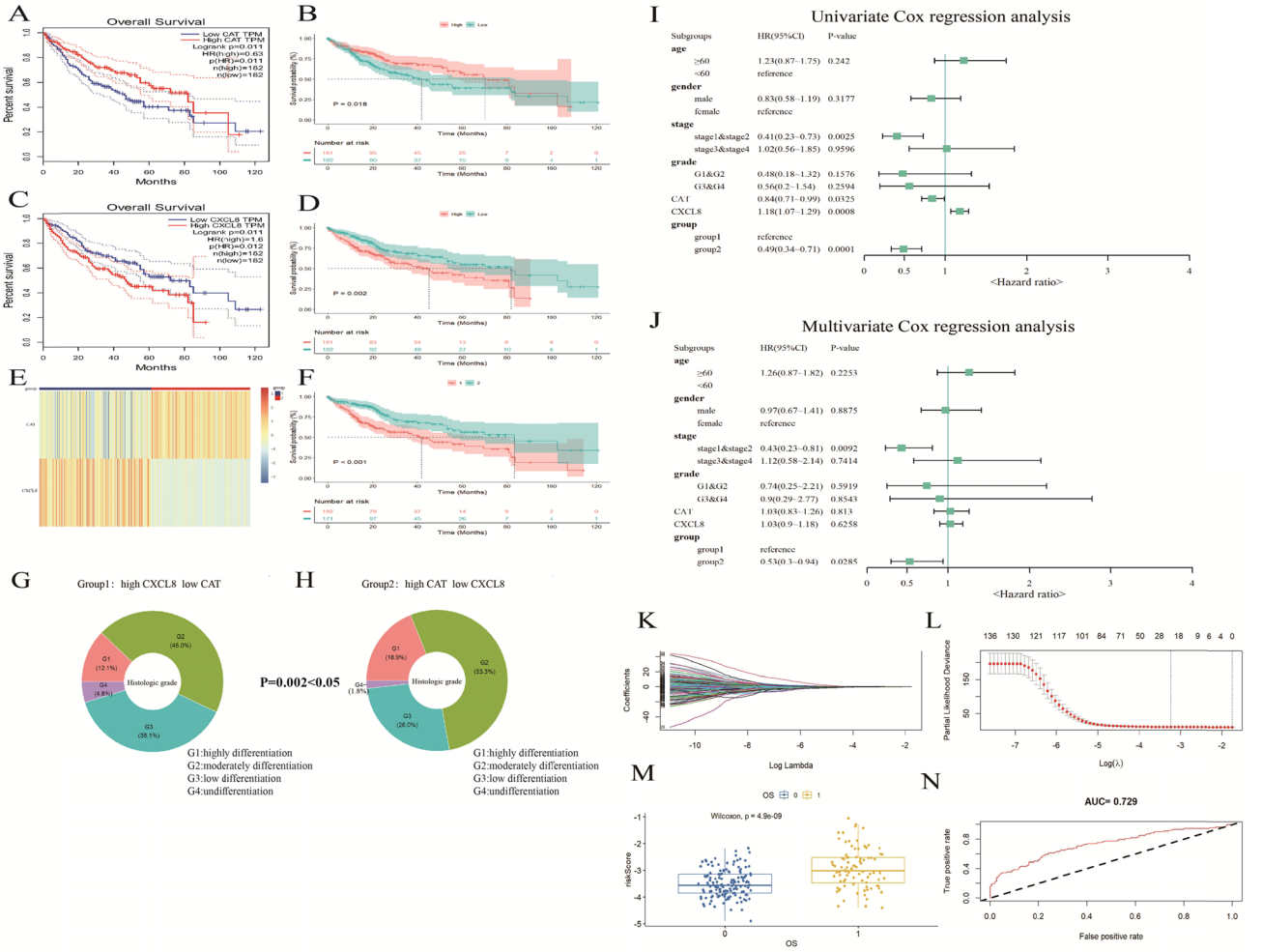

Fig. 4 **A, B** Survival analysis of CAT in liver cancer from GEPIA and TCGA database (MST: high CAT expression = 70.1 months; low CAT expression = 41.8 months); **C, D** Survival analysis of CXCL8 in liver cancer from GEPIA and TCGA database (MST: high CXCL8 expression = 45.1 months; low CXCL8 expression = 81.7 months); **E** Clustering of 363 HCC samples with survival data in TCGA: group 1 (low CAT/high CXCL8; N = 192), group 2 (high CAT/low CXCL8; N = 171); **F** Survival analysis among subgroups in TCGA HCC samples clustering (MST: group 1 = 41.8 months; group 2 = 83.2 months); **G, H** The proportion distribution of histologic grade among subgroups in TCGA HCC samples; **I** Univariate Cox regression analysis with TCGA HCC samples; **J** Multivariate Cox regression analysis with TCGA HCC samples; **K, L** Lasso regression model for CAT and CXCL8; **M** The HCC samples risk score according to the expression level of the CAT and CXCL8; **N** The survival prediction efficacy of the model. (In univariate and multivariate Cox regression analyses, tumour staging was based on the AJCC Version 8 liver cancer staging system.)

By clustering the 363 HCC patients with survival data in TCGA, these samples were divided into two tumour subgroups (Fig. 4E): group 1 included patients with low expression of CAT and high expression of CXCL8, and group 2 included patients with high expression of CAT and low expression of CXCL8. Survival analysis between subgroups was performed, and the results are shown in Fig. 4F. The survival time of HCC patients in group 2 (MST = 83.2 months) was significantly better than that of patients in group 1 (MST = 41.8 months) ($p < 0.001$). The increase in survival time in group 2 (median survival time interval/MSTI = 83.2–41.8 months; 41.4 months) was greater than that in the patients with only high CAT expression or only low CXCL8 expression (MSTI = 70.1–41.8 months; 28.3 months and MSTI = 81.7–45.1 months; 36.6 months). These results further suggest that increased CAT expression might have a protective effect on HCC patients, whereas increased CXCL8 expression might lead to a poor prognosis. The combined use of both CAT and CXCL8 in HCC could better differentiate patients with marked survival benefits.

In addition, the proportion of highly differentiated (grade 1, G1) or moderately differentiated (grade 2, G2) HCCs in group 2 was relatively greater than that in group 1. In other words, the proportion of group 1 with low differentiation (grade 3, G3) or undifferentiation (grade 4, G4) was even greater. The Mann–Whitney U test revealed that the

difference in histological grade between the two groups was statistically significant **(**Fig. 4G, H**)**. These findings suggest that the expression of these two genes also affects the histological differentiation of HCC.

Next, using the clinical data of 363 HCC samples from TCGA, we conducted univariate Cox regression analyses and found that stage 1–2, the CAT expression level, the CXCL8 expression level and group 2 were significantly correlated with the survival of HCC patients. Furthermore, multivariate Cox regression analysis revealed that high CAT/low CXCL8 (group2) was an independent prognostic factor in HCC patients **(**Fig. 4I, J**)**.

In the GEPIA database, genes with positive correlation coefficients ($r \geq 0.5$) with CAT and CXCL8 in TCGA liver cancer samples were screened. As shown in Table 4, 122 CAT-related genes and 15 CXCL8-related genes were included. Using lasso regression, 22 variables were selected to construct a risk score model (Fig. 4K, L). The risk scores were then determined based on the above data. The difference between survival and death risk scores was statistically significant ($P < 0.001$) (Fig. 4M). The discrimination of the risk scores was subsequently assessed using the ROC package in R, which was 0.729, suggesting that the model has good predictive value for mortality risk (Fig. 4N).

3.5 Analysis of immune infiltration in NASH-HCC samples

Cibersort was used to analyse 53 NASH-HCC samples [29], and the results revealed that the microenvironment of NASH-HCC was enriched with activated mast cells, M0 macrophages, follicular helper T cells and naïve B cells, which accounted for a large proportion of the total proportion. These results suggest that these cells play important roles in the progression and development of NASH-HCC (Fig. 5A). The NASH-HCC samples were subsequently clustered according to the combined expression levels of CAT and CXCL8. Similarly, two groups of patients were identified as having NASH-HCC. Group 1 presented low CAT expression and high CXCL8 expression, whereas group 2 presented high CAT expression and low CXCL8 expression (Fig. 5B).

In addition, the Immune Score ($P < 0.001$), Stromal Score ($P < 0.001$), ESTIMATE Score ($P < 0.001$) and Tumour Purity ($P < 0.001$) were significantly different between the two subgroups (Fig. 5C–F). The Immune Score, Stromal Score and ESTIMATE Score in group 1 were significantly greater than those in group 2, but the Tumour Purity was greater in group 2.

Similarly, 363 HCC samples from the TCGA database were analysed using cibersort. The results revealed that the proportions of M1 macrophages, M0 macrophages, monocytes, follicular helper T cells, and naïve CD4 T cells were high in the tumour immune microenvironment (Fig. 5G). The ESTIMATE algorithm revealed that the Immune Score, Stromal Score and ESTIMATE Score in group 1 were significantly greater than those in group 2, but the Tumour Purity was greater in group2**(**Fig. 5I–L**)**, which was the same result as the subgroup comparison of NASH-HCC samples. These results suggested that HCC patients with high CXCL8 expression and low CAT expression had more extensive immune infiltration.

To explore the exact effects of CAT and CXCL8 in HCC, the HCC samples from the TCGA cohort were subsequently analysed based on the tumour subgroups (Fig. 5H) using the xCell algorithm, which is a more comprehensive tool for identifying cell types across the data [35]. The results further revealed that group 1 had higher immune scores (Fig. 5M). However, group 2 had increased naïve CD8 + T cell infiltration ($P < 0.001$).

3.6 Analysis of immune checkpoints and immune therapy effects in different CAT/CXCL8 subgroups

We then explored how CAT and CXCL8 expression was correlated with common immune checkpoints in liver cancer. First, the PDCD1, CTLA4 and CD274 expression levels in NASH-HCC samples did not differ uniformly across the subgroups (Fig. 5B), and only PDCD1 expression was significantly different (Fig. 6A–C). To further clarify this relationship, we compared the expression levels of immune checkpoints among tumour subgroups (Fig. 5H) from the TCGA dataset, the expression levels of PDCD1, CTLA4 and CD274 in group1 (low CAT/high CXCL8) were significantly greater than those in group 2 (high CAT/low CXCL8) consistently (Fig. 6D–F). Through TIDE database analysis, we observed significantly greater TIDE scores, dysfunction scores, and exclusion scores in group 1 than in group 2; however, the MSI score was greater in group 2 (Fig. 6G–J). These findings suggest stronger immune escape and a potentially poor immunotherapy response in group 1.

3.7 Immunohistochemical validation of CAT/CXCL8 expression in NASH-HCC patients from our centre

Among the patients diagnosed with HCC who were hospitalized and underwent surgery in our hospital from 2019 to June 2023, a total of 21 patients with NASH-HCC were screened out according to the latest guideline standards[36] [37], and their clinical data are shown in Table 5. Ten patients with NASH were also included in the control group. The baseline

Table 4 Variables included in the lasso regression risk score model

Genes with positive correlation coefficient r ≥ 0.5 with CAT	Genes with positive correlation coefficient r ≥ 0.5 with CXCL8	Genes(coefficient) that were incorporated into the risk score model
CAT,EHHADH,PIPOX,ACSM2A,GLYATL1,METTL7A,NR1I2,DMGDH,**HAO1**,HSD17B6,SCP2,DNAJC25,GLYAT, ACSM5,**IVD**,PCK2,**ALAD**,GYS2,ACSM2B,**ACBD4**, SARDH,CYB5A,GNE,DAO, ALDH5A1,CGNL1,ABCG8, MPDZ,AADAT,CYP8B1,DCAF11,ALDH6A1,ABAT,PGRMC1,PI4K2B,**TPPP2**,ECI2,ACADL,KNG1,SLC10A1,CMBL,ACAD11,SEPSECS,SORD,EPHX2,ABCG5,**SLC2A2**,PANK1,PEBP1,SLC31A1,MYO1B,ECHDC2,ACOX1,HAGH, HNF4A,**MARC2**,ABCB11,ACADM,MUT,PECR,CYP4F2,**CYP2C8**,SLC6A1,ALDH9A1,AKR1D1,**NDRG2**,XDH,GATM,SELENBP1,**ALDH2**,CYP4A22,PEX19,FMO4,ENTPD5,SERPINC1,TMEM56,ACSL1,BHMT2,IYD,TUBE1,PPARA,**BCKDHB**,SLCO2B1,UPB1,FTCDNL1,**MTTP**,DHTKD1,**CPB2**,C16ORF45,**PBLD**,SLC38A4,N4BP2L1,AR,SLC27A2,CYP4A11,GLYCTK,GBP7,RDH16,ABHD14A-ACY1,ABCA6,**GRHPR**,SMIM14,PIGV,NFIA,MOGAT2,DEPDC7,CYP7A1,SUOX,**CPN2**,KLKB1,CDO1,PGM1,GADD45A,CRY2,EPM2A,MYLK,**NT5DC1**,**RMND5A**,TMBIM6,**THNSL1**,SLC25A20,PEX11G,SPRYD4	**CXCL8**, CXCR2, CXCR1, CEACAM3, CMTM2, CXCL1, ICAM1, ALOX5AP, **FMOD**, **CXCL3**, FFAR2, FAM60A, NFKBIZ, KLHDC7B, RNF145, DENND3	HAO1(-0.115) IVD(-0.004) ALAD(-0.075) ACBD4(-0.047) TPPP2(-0.148) SLC2A2(-0.151) MARC2(-0.198) CYP2C8(-0.001) NDRG2(-0.121) ALDH2(-0.1) BCKDHB(0.054) MTTP(0.131) CPB2(-0.01) PBLD(-0.06) GRHPR(-0.09) CPN2(-0.035) NT5DC1(0.041) RMND5A(0.032) THNSL1(0.476) CXCL8(0.117) FMOD(-0.037) CXCL3(-0.281)

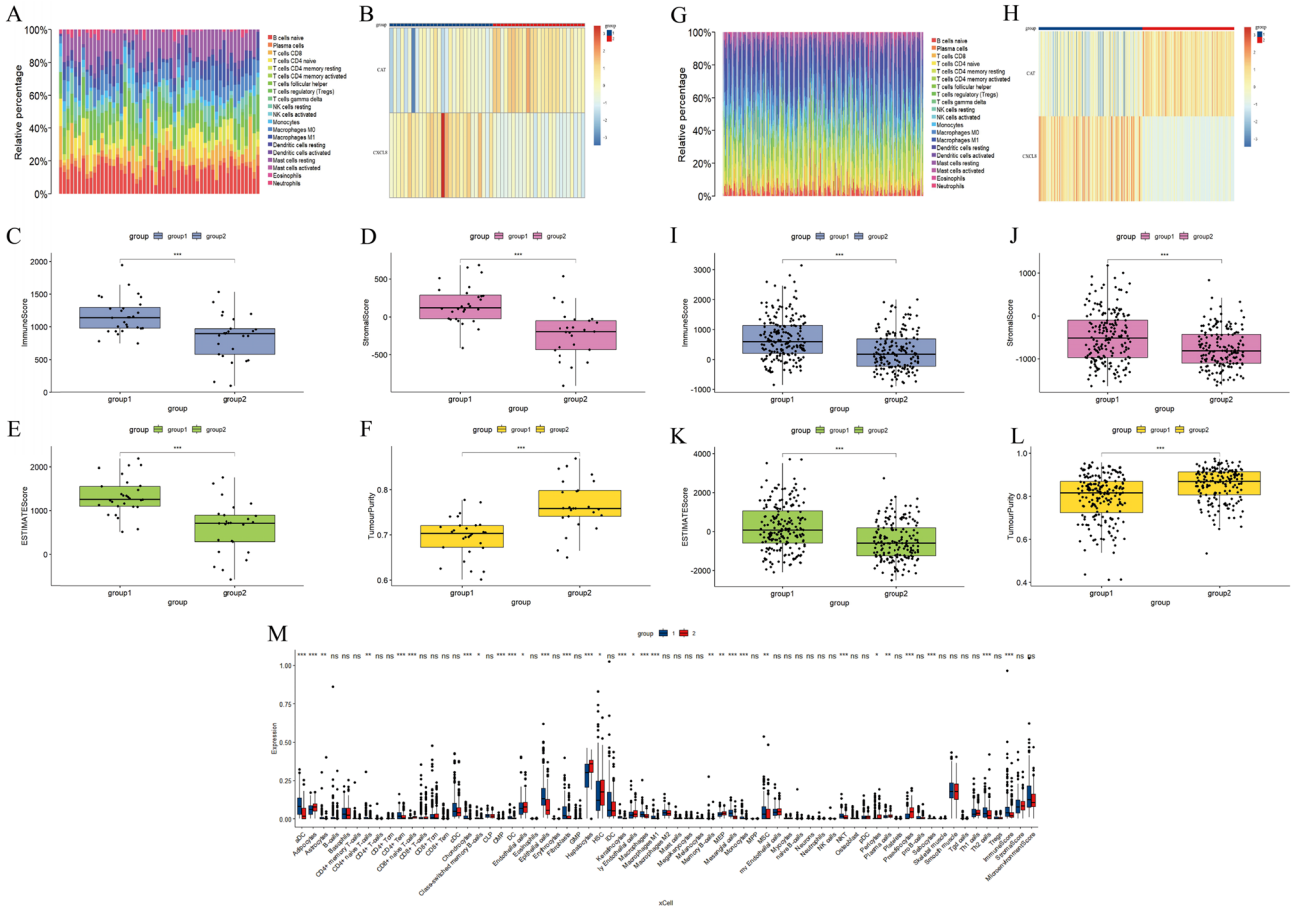

Fig. 5 **A** Proportion of different immune cells in 53 NASH-HCC samples. **B** NASH-HCC samples were clustered into group 1 (N = 28): low CAT expression and high CXCL8 expression; group 2 (N = 25): high CAT expression and low CXCL8 expression. **C–F** Comparison of the ESTIMATE algorithm results in two NASH-HCC subgroups. **G** Proportion of different immune cells in 363 HCC samples from the TCGA database. **H** HCC samples from the TCGA database were clustered into group 1 (N = 192): low CAT expression and high CXCL8 expression; group 2 (N = 171): high CAT expression and low CXCL8 expression; **I–L** Comparison of the ESTIMATE algorithm results in two HCC subgroups from the TCGA database; **M** The characteristics of the immune landscape of the two liver cancer subgroups from the TCGA database were compared using the xCell algorithm. (* means $P < 0.05$; ** means $P < 0.01$; *** means $P < 0.001$.)

clinical data of the patients with NASH and those with NASH-HCC were compared and were not statistically significant (Table 6). Immunohistochemical (IHC) staining was performed on the above NASH-HCC and NASH pathological samples, and the results revealed that the expression of CAT in the NASH group was significantly greater than that in the NASH-related HCC group (Fig. 7A–D), whereas the expression of CXCL8 in the NASH group was significantly lower than that in the NASH-related HCC group (Fig. 7E–H). We subsequently compared the expression of both markers using quantitative IHC staining. The differences among the above groups were statistically significant (Fig. 7I, J). This finding also verified the expression of the above differentially expressed genes: CAT expression was downregulated in NASH-HCC, whereas CXCL8 expression was increased in NASH-HCC.

4 Discussion

NASH has emerged as a major reason for HCC in developed countries [38]. NASH-HCC is a distinct subtype of HCC characterized by its unique pathogenesis and differential response to immunotherapies, some studies have shown that inhibition of cystathionine-gamma-lyase accelerate progression of NASH and may lead to HCC [39]. However, the immune microenvironment in NASH-HCC remains largely undefined. Our findings demonstrate that the differential expression of CAT and CXCL8 significantly impacts immune infiltration levels in both NASH-HCC patients and HCC patients. Specifically, patients with low CAT and high CXCL8 expression (group 1) presented significantly

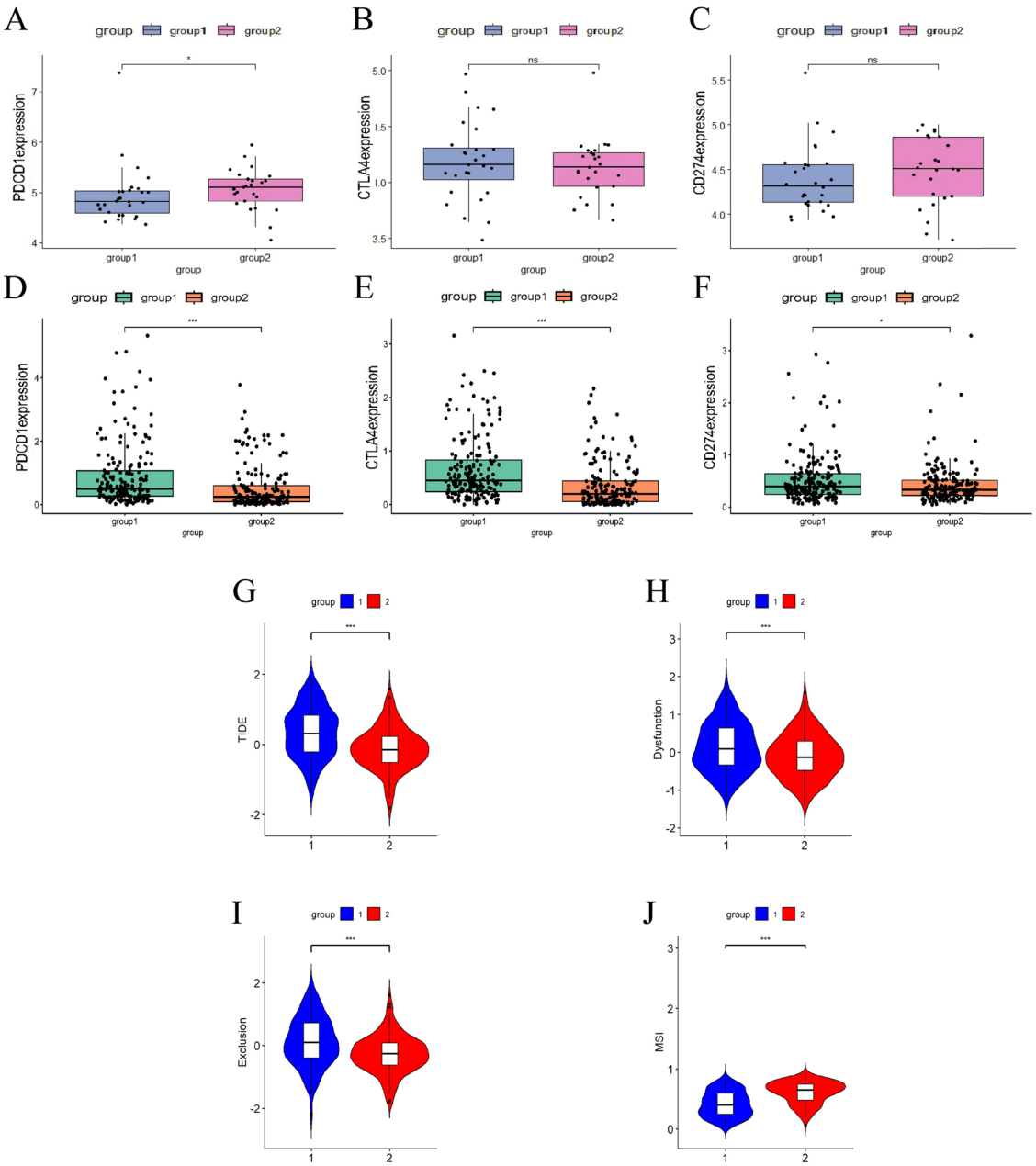

Fig. 6 **A–C** Comparison of the expression levels of PD-1 (PDCD1), CTLA4 and CD274 (PD-L1) in the NASH-HCC subgroups; **D–F** Comparison of the expression levels of PD-1 (PDCD1), CTLA4 and CD274 (PD-L1) in the TCGA HCC subgroups; **G–J** Comparison of the immune therapy effects in the TCGA HCC subgroups (group 1: N = 192; group 2: N = 171; * means $P < 0.05$; ** means $P < 0.01$; *** means $P < 0.001$.)

increased infiltration levels of immune cells compared with those with high CAT and low CXCL8 expression (group 2). Furthermore, among HCC patients, group 1 individuals had a significantly worse prognosis than group 2 individuals, suggesting that CAT and CXCL8 may play important but distinct roles in immune function and patient prognosis.

Malignant tumours are complex entities comprising parenchymal cells, stromal cells, and immune cells. Stromal cells contribute significantly to tumour progression and drug resistance [40–42], whereas intratumoral immune infiltration and level of tumor-associated lymphangiogenesis is closely associated with patient prognosis [43–45]. The ESTIMATE algorithm allows for the inference of infiltrating stromal cells, immune cells, and tumour purity based on gene expression data from tumour samples. In this study, the ESTIMATE results revealed that low CAT expression combined with high CXCL8 expression in both HCC and NASH-HCC led to increased levels of infiltrating immune

Table 5 Clinical characteristics of 21 NASH-HCC patients in the validation dataset

Characteristics	Groups	Cases (N = 21)	Proportion (%)
Gender	Male	16	76.2
	Female	5	23.8
Age	< 60	3	14.3
	≥ 60	18	85.7
BCLC Stage	A	18	85.7
	B	3	14.3
	C	0	0
	D	0	0
Liver cirrhosis	Yes	9	42.9
	No	12	57.1
AFP(ng/mL)	< 7	10	47.6
	7–400	8	38.1
	> 400	3	14.3
TBIL(μmol/L)	< 24	18	85.7
	≥ 24	3	14.3
ALB(g/L)	< 28	1	4.8
	28–35	1	4.8
	> 35	19	90.5
ALT(U/L)	< 50	21	100
	≥ 50	0	0
AST	< 40	19	90.5
	≥ 40	2	9.5
Child–Pugh grade	A	18	85.7
	B	3	14.3
	C	0	0

Table 6 Comparison of clinical parameters between 10 NASH patients and 21 NASH-HCC patients

Clinical parameters	NASH(N = 10)	NASH HCC(N = 21)	P-value
Gender (male:female)	7:3	16:5	0.724
Age (year)	62.20 ± 7.36	67.81 ± 8.93	0.096
ALT (U/L)	24.13 ± 7.66	21.97 ± 9.80	0.545
AST (U/L)	24.75 ± 10.11	27.57 ± 14.75	0.590
TBIL (μmol/L)	13.44 ± 7.84	16.19 ± 17.2	0.636
ALB (g/L)	40.96 ± 3.09	39.67 ± 6.18	0.539
Child–Pugh grade	5.40 ± 0.84	5.38 ± 0.86	0.954

cells and stromal cells but decreased tumour purity (Fig. 5C–F, I–L). Notably, the prognosis of HCC patients strongly correlates with the intratumoral infiltration levels of both immune cells and stromal components.

In the TCGA HCC samples analysed, we observed consistently increased levels of immune infiltration within the high CXCL8/low CAT group; however, naïve CD8 + T cells, which play a predominant role in antitumour immunity [46, 47], were significantly reduced (Fig. 5M). The increased expression of CXCL8 indicates enhanced and more complex immune infiltration, whereas the increased expression of CAT within tumour tissues represents a distinct signature of antitumour naïve CD8 + T cells. Therefore, patients with higher CAT but lower CXCL8 levels in HCC have a significantly better prognosis, suggesting an important role for pure antitumour naïve CD8 + T cell signatures.

The presence of ROS induces DNA damage and genomic instability, leading to carcinogenic effects [48, 49]. Consequently, cancer cells typically exhibit higher levels of ROS than noncancer cells do. Some studies have demonstrated that CXCL8 is enriched in the microenvironment of HCC and promotes HCC angiogenesis through the STAT3 signalling pathway, thereby facilitating tumour growth and invasion. Furthermore, as depicted in Fig. 5M, M1 macrophage infiltration was greater in the group with high expression of CXCL8 because of the ability of M1 macrophages to stimulate an

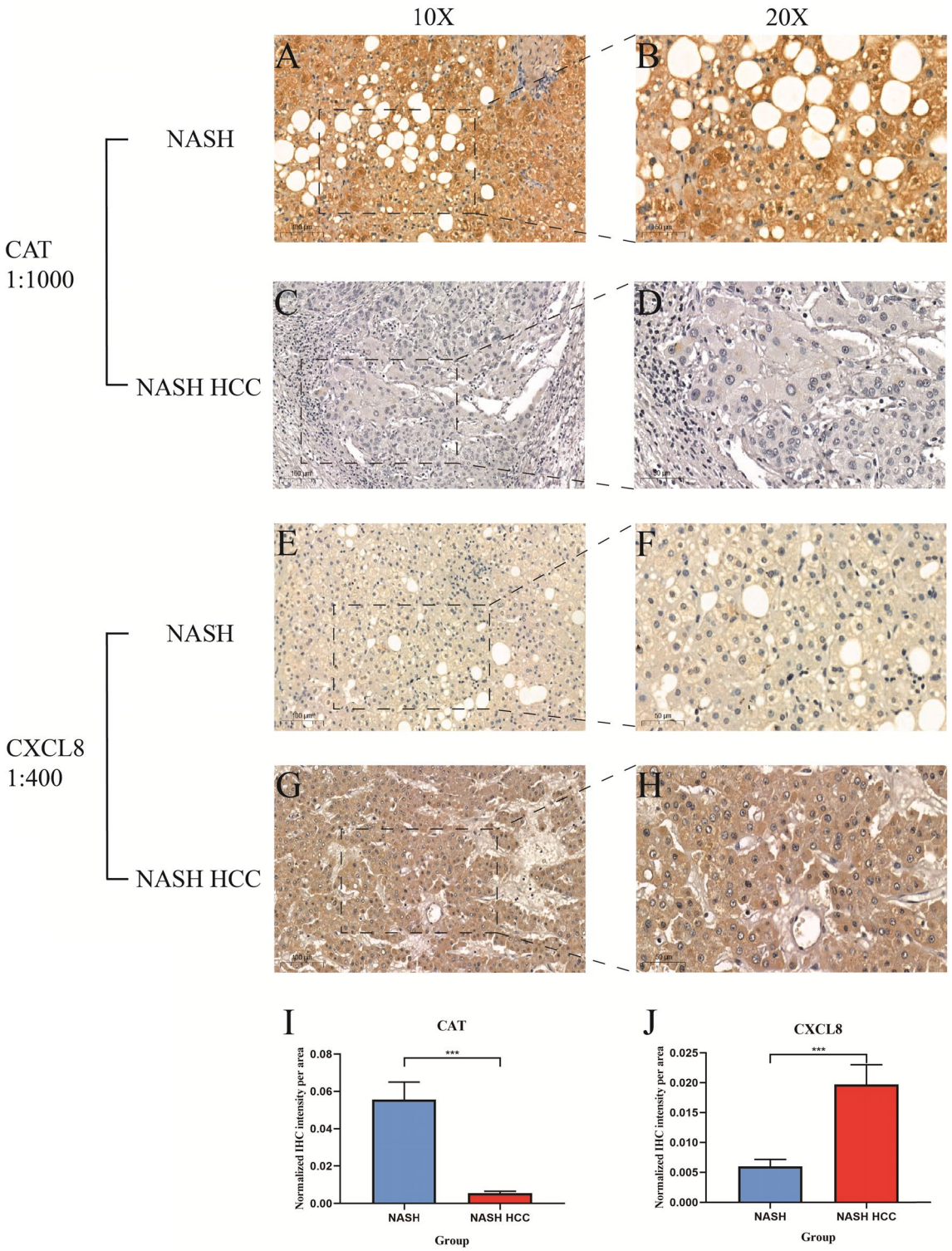

Fig. 7 IHC staining analysis of CAT and CXCL8 in NASH and NASH-HCC samples from our centre. NASH pathological samples stained with CAT antibody, imaged at 10X (**A**) and 20X (**B**); NASH-HCC pathological samples stained with CAT antibody, imaged at 10X (**C**) and 20X (**D**); NASH pathological samples stained with 1:400 CXCL8 antibody, imaged at 10X (**E**) and 20X (**F**); NASH-HCC pathological samples stained with 1:400 CXCL8 antibody, imaged at 10X (**G**) and 20X (**H**); **I** Comparison of CAT normalized immunohistochemical intensity between the NASH group (N = 10) and the NASH-HCC group (N = 21); **J** Comparison of CXCL8 normalized immunohistochemical intensity between the NASH group (N = 10) and the NASH-HCC group (N = 21); (* means $P < 0.05$; ** means $P < 0.01$; *** means $P < 0.001$. The experiment was repeated three times for each sample, and the mean IHC intensity was used for statistical analysis)

increase in ROS levels. Therefore, CXCL8 can promote tumour invasion by accelerating angiogenesis and increasing ROS levels [50]. CAT plays a crucial role in maintaining DNA stability and limiting tumour progression by decomposing ROS; moreover, CAT has been shown to inhibit CXCL8 mRNA expression [51]. In this way, CAT improves HCC prognosis not only by simplifying immune infiltration but also by decomposing ROS and suppressing CXCL8 expression.

As mentioned above, CAT can decompose ROS, which can increase tumour cell survival, proliferation, metastasis, drug resistance and other functions in various types of cancers [52–57]. Notably, among mammals, liver and blood cells exhibit the highest activity level of CAT [58, 59]. On the other hand, CXCL8 acts as an inflammatory chemokine that regulates intricate immune cell infiltration which may impede antitumour immune responses within the microenvironment [60–62].

Based on our discussion above, this study revealed a strong correlation between the effect of CAT and that of CXCL8. By comparing the expression levels of three common immune checkpoints, CD274 (PD-L1), PDCD1, and CTLA4, between the two subgroups of HCC patients (Fig. 6D–F), we observed that low CAT expression combined with high CXCL8 expression indicates a potentially stronger role for tumour immune escape, resulting in tumour progression and poor prognosis. Therefore, despite the poor prognosis of HCC patients, low CAT and high CXCL8 expression can be used to screen for patient subgroups more suitable for certain immunotherapies based on the TIDE score (Fig. 6G–J).

However, there are still several limitations in this study. First, this study investigated only the correlation between CAT and CXCL8 in antitumour immune infiltration without delving into the underlying mechanisms involved. Second, further experiments are needed to validate the survival outcomes and immune infiltration of liver cancer patients with or without NASH separately. Therefore, follow-up studies are needed to obtain survival data for NASH-HCC patients and determine whether the impact of CAT and CXCL8 on their prognosis aligns with the findings of this study. Overall, additional validation is necessary to elucidate how these two genes interact to influence NASH-HCC development, immune infiltration and the prognosis of HCC patients. This approach will enable subclassification of HCC patients for optimal efficacy of specific immunotherapies.

5 Conclusion

CAT and CXCL8 play pivotal roles in the progression of NASH-HCC patients. HCC patients with low CAT and high CXCL8 expression may have stronger immune infiltration and stronger tumour immune escape. However, possibly due to its different effects on CD8 + T cells and reactive oxygen species production, CAT can improve the prognosis of liver cancer patients, whereas CXCL8 leads to a poorer prognosis.

Acknowledgements We are grateful to the patients who provided the pathological specimens, our peers for sharing the sample data and survival data.

Author contributions All the authors contributed to the study conception and design. Material preparation, data collection and analysis were performed by L Y, P L and J Z. L Y and Z B and G Z conducted the visualization. The first draft of the manuscript was written by L Y and P L. X L, B Z and J L revised the manuscript. All the authors have read and approved the final manuscript.

Funding This work was supported by the National Natural Science Foundation of China (grant numbers 81971773 and 82272105) and the Guangdong Basic and Applied Basic Research Foundation (grant numbers 2022A1515011244, 2022A1515012382, 2023A1515010475, and 2023A1515011521).

Data availability Publicly available datasets were analysed in this study. The dataset supporting this study is available from (https://xenabrowser.net/datapages/) and the GEO database(https://www.ncbi.nlm.nih.gov/geo/). The validation datasets are available from the corresponding author upon reasonable request.

Declarations

Ethics approval and consent to participate The protocol was approved by the Research Ethics Committee of the 5th Affiliated Hospital of Sun Yat-sen University (reference number 2022-L409-1) in accordance with the Declaration of Helsinki 1964 or equivalent ethical principles. Informed consent was obtained from all individual participants included in the study.

Competing interests The authors declare no competing interests.

References

1. Calderaro J, et al. Artificial intelligence for the prevention and clinical management of hepatocellular carcinoma. J Hepatol. 2022;76(6):1348–61.
2. Pinter M, et al. NASH and hepatocellular carcinoma: immunology and immunotherapy. Clin Cancer Res. 2023;29(3):513–20.
3. Forner A, Llovet JM, Bruix J. Hepatocellular carcinoma. Lancet. 2012;379(9822):1245–55.
4. Hsu YC, et al. Therapeutic effects of Anti-PD1 immunotherapy on hepatocellular carcinoma under administration of tacrolimus. Transplantation. 2022. https://doi.org/10.1097/TP.0000000000004425.
5. Wong RJ, Cheung R, Ahmed A. Nonalcoholic steatohepatitis is the most rapidly growing indication for liver transplantation in patients with hepatocellular carcinoma in the U.S. Hepatology. 2014;59(6):2188–95.
6. Margini C, Dufour JF. The story of HCC in NAFLD: from epidemiology, across pathogenesis, to prevention and treatment. Liver Int. 2016;36(3):317–24.
7. Adams LA, et al. The natural history of nonalcoholic fatty liver disease: a population-based cohort study. Gastroenterology. 2005;129(1):113–21.
8. White DL, Kanwal F, El-Serag HB. Association between nonalcoholic fatty liver disease and risk for hepatocellular cancer, based on systematic review. Clin Gastroenterol Hepatol. 2012;10(12):1342-1359.e2.
9. Cheng AL, et al. Updated efficacy and safety data from IMbrave150: Atezolizumab plus bevacizumab vs. sorafenib for unresectable hepatocellular carcinoma. J Hepatol. 2022;76(4):862–73.
10. Finn RS, et al. IMbrave150: Updated overall survival (OS) data from a global, randomized, open-label phase III study of atezolizumab (atezo) + bevacizumab (bev) versus sorafenib (sor) in patients (pts) with unresectable hepatocellular carcinoma (HCC). J Clin Oncol. 2021;39(3_suppl):267–267.
11. Pfister D, et al. NASH limits anti-tumour surveillance in immunotherapy-treated HCC. Nature. 2021;592(7854):450–6.
12. Wolf MJ, et al. Metabolic activation of intrahepatic CD8+ T cells and NKT cells causes nonalcoholic steatohepatitis and liver cancer via cross-talk with hepatocytes. Cancer Cell. 2014;26(4):549–64.
13. Wu J, et al. The proinflammatory myeloid cell receptor TREM-1 controls Kupffer cell activation and development of hepatocellular carcinoma. Cancer Res. 2012;72(16):3977–86.
14. Ju C, Tacke F. Hepatic macrophages in homeostasis and liver diseases: from pathogenesis to novel therapeutic strategies. Cell Mol Immunol. 2016;13(3):316–27.
15. Malehmir M, et al. Platelet GPIbα is a mediator and potential interventional target for NASH and subsequent liver cancer. Nat Med. 2019;25(4):641–55.
16. Donne R, Lujambio A. The liver cancer immune microenvironment: therapeutic implications for hepatocellular carcinoma. Hepatology. 2022. https://doi.org/10.1002/hep.32740.
17. Llovet JM, et al. Immunotherapies for hepatocellular carcinoma. Nat Rev Clin Oncol. 2022;19(3):151–72.
18. Barek MA, et al. Catalase C262T genetic variation and cancer susceptibility: a comprehensive meta-analysis with meta-regression and trial sequential analysis. Int J Biol Markers. 2022;37(3):227–40.
19. Glorieux C, Calderon PB. Catalase, a remarkable enzyme: targeting the oldest antioxidant enzyme to find a new cancer treatment approach. Biol Chem. 2017;398(10):1095–108.
20. Najafi A, et al. Catalase application in cancer therapy: Simultaneous focusing on hypoxia attenuation and macrophage reprogramming. Biomed Pharmacother. 2022;153: 113483.
21. Waugh DJ, Wilson C. The interleukin-8 pathway in cancer. Clin Cancer Res. 2008;14(21):6735–41.
22. Azenshtein E, et al. The angiogenic factors CXCL8 and VEGF in breast cancer: regulation by an array of pro-malignancy factors. Cancer Lett. 2005;217(1):73–86.
23. Ferrer FA, et al. Angiogenesis and prostate cancer: in vivo and in vitro expression of angiogenesis factors by prostate cancer cells. Urology. 1998;51(1):161–7.
24. Kim SJ, et al. Expression of interleukin-8 correlates with angiogenesis, tumorigenicity, and metastasis of human prostate cancer cells implanted orthotopically in nude mice. Neoplasia. 2001;3(1):33–42.
25. Pine SR, et al. Increased levels of circulating interleukin 6, interleukin 8, C-reactive protein, and risk of lung cancer. J Natl Cancer Inst. 2011;103(14):1112–22.
26. Balasoiu M, et al. Serum and tumor microenvironment IL-8 values in different stages of colorectal cancer. Rom J Morphol Embryol. 2014;55(2 Suppl):575–8.
27. Han ZJ, et al. Roles of the CXCL8-CXCR1/2 axis in the tumor microenvironment and immunotherapy. Molecules. 2021. https://doi.org/10.3390/molecules27010137.
28. Marcil V, et al. Modification in oxidative stress, inflammation, and lipoprotein assembly in response to hepatocyte nuclear factor 4alpha knockdown in intestinal epithelial cells. J Biol Chem. 2010;285(52):40448–60.
29. Pinyol R, et al. Molecular characterisation of hepatocellular carcinoma in patients with non-alcoholic steatohepatitis. J Hepatol. 2021;75(4):865–78.
30. Qian L, et al. In silico identification and verification of Tanshinone IIA-related prognostic genes in hepatocellular carcinoma. Front Immunol. 2024;15:1482914.

31. Hu W, Fang T, Chen X. Identification of differentially expressed genes and miRNAs for ulcerative colitis using bioinformatics analysis. Front Genet. 2022;13: 914384.
32. Du LJ, Song YH, Tang LX. Effect of acute exercise on gene expression in peripheral blood mononuclear cells of puberty children. Sci Rep. 2024;14(1):27977.
33. Tang Z, et al. GEPIA: a web server for cancer and normal gene expression profiling and interactive analyses. Nucleic Acids Res. 2017;45(W1):W98-w102.
34. Jiang P, et al. Signatures of T cell dysfunction and exclusion predict cancer immunotherapy response. Nat Med. 2018;24(10):1550–8.
35. Aran D, Hu Z, Butte AJ. xCell: digitally portraying the tissue cellular heterogeneity landscape. Genome Biol. 2017;18(1):220.
36. Eslam M, et al. A new definition for metabolic dysfunction-associated fatty liver disease: an international expert consensus statement. J Hepatol. 2020;73(1):202–9.
37. Udoh UA, et al. Non-alcoholic fatty liver disease progression to non-alcoholic steatohepatitis-related primary liver cancer. In: Sergi CM, editor., et al., Liver cancer. Brisbane: Exon Publications; 2021.
38. Peng B, Ge Y, Yin G. A novel prognostic gene signature, nomogram and immune landscape based on tanshinone IIA drug targets for hepatocellular carcinoma: Corehensive bioinformatics analysis and in vitro experiments. Biocell. 2023;47(7):1519–35.
39. Ma Y, Wang S, Ding H. Bioinformatics analysis and experimental validation of cystathionine-gamma-lyase as a potential prognosis biomarker in hepatocellular carcinoma. Biocell. 2024;48(3):463–71.
40. Hanahan D, Weinberg RA. Hallmarks of cancer: the next generation. Cell. 2011;144(5):646–74.
41. Kalluri R, Zeisberg M. Fibroblasts in cancer. Nat Rev Cancer. 2006;6(5):392–401.
42. Straussman R, et al. Tumour micro-environment elicits innate resistance to RAF inhibitors through HGF secretion. Nature. 2012;487(7408):500–4.
43. Fridman WH, et al. The immune contexture in cancer prognosis and treatment. Nat Rev Clin Oncol. 2017;14(12):717–34.
44. Pages F, et al. International validation of the consensus Immunoscore for the classification of colon cancer: a prognostic and accuracy study. Lancet. 2018;391(10135):2128–39.
45. Li J, et al. Tumor-associated lymphatic vessel density is a reliable biomarker for prognosis of esophageal cancer after radical resection: a systemic review and meta-analysis. Front Immunol. 2024;15:1453482.
46. MacNabb BW, et al. Dendritic cells can prime anti-tumor CD8(+) T cell responses through major histocompatibility complex cross-dressing. Immunity. 2022;55(6):982-997.e8.
47. Bae EA, et al. Activation of NKT cells in an anti-PD-1-resistant tumor model enhances antitumor immunity by reinvigorating exhausted CD8 T cells. Cancer Res. 2018;78(18):5315–26.
48. Radisky DC, et al. Rac1b and reactive oxygen species mediate MMP-3-induced EMT and genomic instability. Nature. 2005;436(7047):123–7.
49. Nieborowska-Skorska M, et al. Rac2-MRC-cIII-generated ROS cause genomic instability in chronic myeloid leukemia stem cells and primitive progenitors. Blood. 2012;119(18):4253–63.
50. Yao C, et al. Angiogenesis in hepatocellular carcinoma: mechanisms and anti-angiogenic therapies. Cancer Biol Med. 2023;20(1):25–43.
51. Ishikawa S, et al. Heme induces DNA damage and hyperproliferation of colonic epithelial cells via hydrogen peroxide produced by heme oxygenase: a possible mechanism of heme-induced colon cancer. Mol Nutr Food Res. 2010;54(8):1182–91.
52. Moloney JN, Cotter TG. ROS signalling in the biology of cancer. Semin Cell Dev Biol. 2018;80:50–64.
53. Sullivan LB, Chandel NS. Mitochondrial reactive oxygen species and cancer. Cancer Metab. 2014;2:17.
54. Dalla Pozza E, et al. Role of mitochondrial uncoupling protein 2 in cancer cell resistance to gemcitabine. Biochim Biophys Acta. 2012;1823(10):1856–63.
55. Donadelli M, et al. Synergistic inhibition of pancreatic adenocarcinoma cell growth by trichostatin A and gemcitabine. Biochim Biophys Acta. 2007;1773(7):1095–106.
56. Wu WS, et al. Reactive oxygen species mediated sustained activation of protein kinase C alpha and extracellular signal-regulated kinase for migration of human hepatoma cell Hepg2. Mol Cancer Res. 2006;4(10):747–58.
57. Wu WS. The signaling mechanism of ROS in tumor progression. Cancer Metastasis Rev. 2006;25(4):695–705.
58. Winternitz MC, Meloy CR. On the occurrence of catalase in human tissues and its variations in diseases. J Exp Med. 1908;10(6):759–81.
59. Mueller S, Riedel HD, Stremmel W. Direct evidence for catalase as the predominant H2O2 -removing enzyme in human erythrocytes. Blood. 1997;90(12):4973–8.
60. Rosenkilde MM, Schwartz TW. The chemokine system—a major regulator of angiogenesis in health and disease. APMIS. 2004;112(7–8):481–95.
61. Verbeke H, et al. The role of CXC chemokines in the transition of chronic inflammation to esophageal and gastric cancer. Biochim Biophys Acta. 2012;1825(1):117–29.
62. Heidemann J, et al. Angiogenic effects of interleukin 8 (CXCL8) in human intestinal microvascular endothelial cells are mediated by CXCR2. J Biol Chem. 2003;278(10):8508–15.